



云南大学中国西南天文研究所  
South-Western Institute For Astronomy Research, YNU

# A machine-learning photometric classifier for massive stars in nearby galaxies II. The catalog

G. Maravelias<sup>1,2</sup>, A. Z. Bonanos<sup>1</sup>, K. Antoniadis<sup>1,3</sup>, G. Munoz-Sanchez<sup>1,3</sup>, E. Christodoulou<sup>1,3</sup>, S. de Wit<sup>1</sup>, E. Zapartas<sup>2</sup>, K. Kovlakas<sup>4,5</sup>, F. Tramper<sup>6</sup>, P. Bonfini<sup>7,8</sup>, and S. Avgousti<sup>9</sup>

<sup>1</sup> IAASARS, National Observatory of Athens, GR-15236, Penteli, Greece

<sup>2</sup> Institute of Astrophysics, FORTH, GR-71110, Heraklion, Greece

<sup>3</sup> Department of Physics, National and Kapodistrian University of Athens, Panepistimiopolis, GR-15784, Zografos, Greece

<sup>4</sup> Institute of Space Sciences (ICE), CSIC, Campus UAB, E-08193, Barcelona, Spain

<sup>5</sup> Institut d'Estudis Espacials de Catalunya (IEEC), Edifici RDIT, Campus UPC, E-08860, Castelldefels (Barcelona), Spain

<sup>6</sup> Centro de Astrobiología (CSIC-INTA), E-28850, Torrejón de Ardoz, Spain

<sup>7</sup> Alma-Sistemi Srl, IT-00012 Guidonia, Italy

<sup>8</sup> Physics Department, and Institute of Theoretical and Computational Physics, University of Crete, GR-71003 Heraklion, Greece

<sup>9</sup> Department of Informatics and Telecommunications, National and Kapodistrian University of Athens, GR-16122, Greece

**Reporter: Baisong Zhang (张百松)**

**2025-05-30**

# 1. Introduction

- One of the main goals of JWST is to study galaxies over cosmic time, from the early Universe to now.
- Massive stars
  - Through their feedback, whether from strong stellar winds or explosive supernovae, massive stars play a critical role in enriching and shaping the environments of their host galaxies.
  - This is especially important in the early Universe, when metallicity was extremely low and the formation and evolution of such stars is still not well understood.
- The only way to gain insight into these objects is by examining these populations in nearby low metallicity galaxies.
- Resolved population studies in such galaxies are possible in the Local Group (*e.g. Sextans A; Lorenzo et al. 2022, LMC; Vink et al. 2023, SMC; Shenar et al. 2024*) but challenging at larger distances.
- Therefore, we lack well-explored populations of massive stars at these metallicities.

# 1. Introduction

- The main goal of the ASSESS1 ("Episodic Mass Loss in Evolved Massive stars: Key to Understanding the Explosive Early Universe") project ([\*Bonanos et al. 2024\*](#)) was to investigate the role of episodic mass loss in the evolution of massive stars ([\*see e.g. Yang et al. 2023; Antoniadis et al. 2024, 2025; de Wit et al. 2024; Munoz-Sanchez et al. 2024a,b; Zapartas et al. 2024\*](#)).
- A large number of sources with secure classifications was needed to explore its importance across various metallicity environments, therefore we set up both an observing campaign to acquire spectra for a large number of sources ([\*see e.g. de Wit et al. 2023; Bonanos et al. 2024; de Wit et al., subm.\*](#)) as well as a machine-learning approach ([\*Maravelias et al. 2022; henceforth Paper I\*](#)).

# 1. Introduction

- We developed a classifier that uses optical and IR photometry to select dusty, mass losing, evolved massive stars and classify Spitzer detected point sources into different broad classes.
  - The purpose of this classifier was to predict the classes for approximately 1.2 M sources from 26 galaxies within 5 Mpc and spanning a metallicity range ( $0.07-1.36 Z_{\odot}$ ), creating the largest point-source catalog with spectral-type classifications for and beyond the Local Group.

## 2. Data collection and processing

- 2.1. Galaxy sample
  - We present the results of applying the classifier to the whole sample of galaxies included in the ASSESS project ([Bonanos et al. 2024](#)) (except for the LMC and SMC which were treated separately, e.g. [Yang et al. 2019, 2020, 2021, 2023](#); [de Wit et al. 2023](#); [Antoniadis et al. 2024](#); [Munoz-Sanchez et al. 2024a](#)).

## 2. Data collection and processing

**Table 1.** Galaxies examined in this work along with some basic properties.

Galaxy	R.A. (J2000) (hh:mm:ss)	Dec. (J2000) (dd:mm:ss)	Type <sup>a</sup>	Radius ( $'$ )	Distance <sup>b</sup> (Mpc)	Metallicity <sup>c</sup> ( $Z_{\odot}$ )
WLM	00:01:58	−15:27:39	SB(s)m: sp	9	0.95±0.01	0.13 <sup>1</sup>
NGC 55	00:14:54	−39:11:48	SB(s)m? edge-on	21	1.98±0.02	0.31 <sup>2</sup>
IC 10	00:20:17	+59:18:14	dIrr IV/BCD	6	0.78±0.04	0.47 <sup>3</sup>
M31	00:42:44	+41:16:09	SA(s)b LINER	105	0.75±0.02	1.36 <sup>4</sup>
NGC 247	00:47:09	−20:45:37	SAB(s)d	14	3.56±0.03	0.54 <sup>5</sup>
NGC 253	00:47:33	−25:17:18	SAB(s)c	21	3.61±0.03	0.83 <sup>6</sup>
NGC 300	00:54:53	−37:41:04	SA(s)d	15	1.94±0.04	0.41 <sup>7</sup>
IC 1613	01:04:48	+02:07:04	IB(s)m	14	0.72±0.01	0.16 <sup>8</sup>
M33	01:33:51	+30:39:37	SA(s)cd HII	30	0.85±0.02	0.65 <sup>9</sup>
Phoenix Dwarf	01:51:06	−44:26:41	IAm	8	0.43±0.01	0.07 <sup>10</sup>
NGC 1313	03:18:16	−66:29:54	SB(s)d	8	4.21±0.06	0.35 <sup>11</sup>
NGC 2366	07:28:55	+69:12:57	IB(s)m	6	3.21±0.04	0.16 <sup>12</sup>
NGC 2403	07:36:51	+65:36:09	SAB(s)cd	14	3.13±0.06	0.56 <sup>13</sup>
M81	09:55:33	+69:03:55	SA(s)ab	18	3.61±0.22	0.60 <sup>14</sup>
Sextans B	10:00:00	+05:19:56	IB(s)m	5	1.38±0.08	0.10 <sup>15</sup>
NGC 3109	10:03:07	−26:09:35	SB(s)m edge-on	13	1.37±0.08	0.12 <sup>16</sup>
NGC 3077	10:03:19	+68:44:02	I0 pec	5	3.75±0.11	0.89 <sup>17</sup>
Sextans A	10:11:01	−04:41:34	IBm	4	1.41±0.05	0.07 <sup>15</sup>
NGC 4214	12:15:39	+36:19:37	IAB(s)m	7	2.82±0.09	0.32 <sup>18</sup>
NGC 4736	12:50:53	+41:07:14	(R)SA(r)ab	11	4.34±0.08	0.48 <sup>19</sup>
NGC 4826	12:56:44	+21:40:59	(R)SA(rs)ab	7	4.36±0.06	0.22 <sup>20</sup>
M83	13:37:01	−29:51:56	SAB(s)c	10	4.79±0.09	0.97 <sup>21</sup>
NGC 5253	13:39:56	−31:38:24	Im pec	4	3.55±0.21	0.37 <sup>22</sup>
NGC 6822	19:44:58	+14:48:12	IB(s)m	10	0.46±0.01	0.30 <sup>23</sup>
Pegasus DIG	23:28:36	+14:44:35	dI	8	0.95±0.03	0.10 <sup>24</sup>
NGC 7793	23:57:50	+32:35:28	SA(s)d	8	3.39±0.06	0.48 <sup>25</sup>

The basic properties of the galaxies, including their names, coordinates, types, radii (which correspond to the sizes of the galaxy based on visual inspection that was used to match the catalogs), distances, and metallicity.

## 2. Data collection and processing

- 2.2. Surveys used and data processing
  - IR photometry: we based our catalogs on precompiled point-source catalogs from the Spitzer Space Telescope ([Boyer et al. 2015](#); [Khan et al. 2015](#); [Khan 2017](#); [Williams & Bonanos 2016](#)).
  - The mid-IR photometry (3.6  $\mu\text{m}$ , 4.5  $\mu\text{m}$ , 5.8  $\mu\text{m}$ , 8.0  $\mu\text{m}$ , 24  $\mu\text{m}$  ) was cross-matched with optical photometry (g,r, i,z, y) obtained from the Pan-STARRS1([Chambers et al. 2016](#)) or PS1 data archive, which is not available for the most southern galaxies.
  - Additional photometry was obtained from the VISTA Hemisphere Survey (VHS; [McMahon 2012](#)), and the UK InfraRed Telescope (UKIRT) Hemisphere Survey (UHS; [Dye et al. 2018](#); [Irwin 2013](#)), with a limited, however, coverage of our sample for each survey



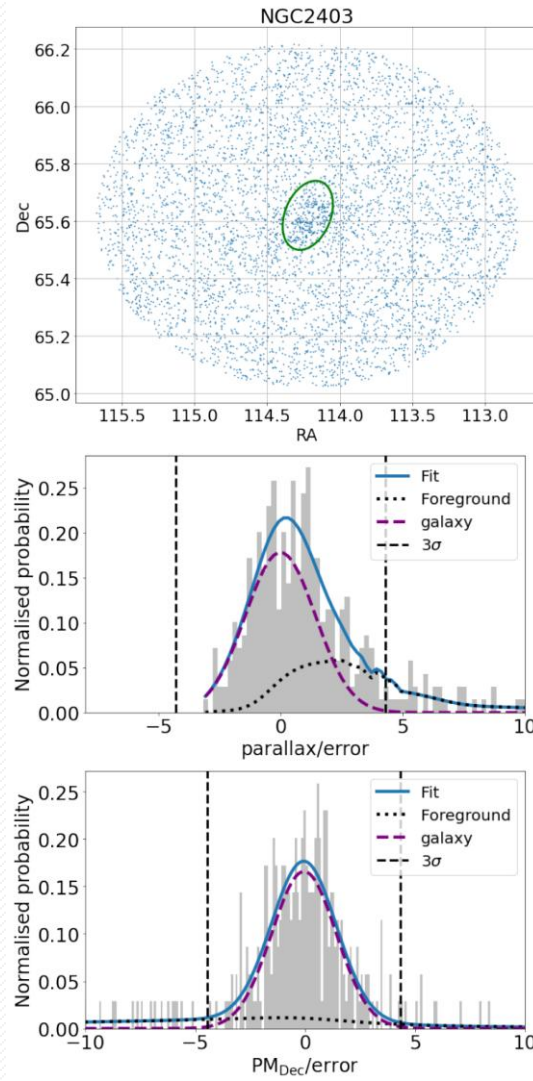
## • 2.3. Removing foreground stars---Gaia DR3 astrometry was used to remove foreground sources.

**Table 2.** Number of sources per photometric survey and foreground selection criteria per galaxy. The columns contain the initial number of *Spitzer* sources as well as their cross-matches with Pan-STARRS, *Gaia*, UHS, and VHS. Parallax and proper motion limits for foreground detection are provided, before the final number of sources after removing duplicate sources.

Galaxy	<i>Spitzer</i>	PS-DR1	<i>Gaia</i> -DR3	UHS	VHS	Parallax/error	pmRA/error	pmDec/error	Selected	Final
WLM	14234	3331	399	0	3291	$-0.08 \pm 0.99$	$0.26 \pm 1.20$	$-0.10 \pm 1.11$	14091	13139
NGC 55	8698	0	729	0	0	$-0.06 \pm 1.13$	$0.02 \pm 1.20$	$0.06 \pm 1.49$	8524	8496
IC 10	32901	4547	1931	6006	0	$-0.16 \pm 1.12^*$	$0.09 \pm 1.15^*$	$-0.13 \pm 1.27^*$	31673	29499
M31	815811	410634	26332	387613	0	$-0.16 \pm 1.12$	$0.09 \pm 1.15$	$-0.13 \pm 1.27$	809142	809052
NGC 247	13398	2470	621	0	0	$0.01 \pm 0.85$	$0.21 \pm 0.98$	$-0.03 \pm 1.14$	13095	13095
NGC 253	8734	1578	522	0	0	$0.06 \pm 1.20$	$-0.00 \pm 1.07$	$0.02 \pm 1.31$	8409	8381
NGC 300	20511	0	1400	0	11480	$0.00 \pm 1.20$	$0.14 \pm 1.12$	$-0.12 \pm 1.23$	20161	20153
IC 1613	28371	10364	1229	0	0	$-0.18 \pm 0.96$	$0.11 \pm 1.03$	$-0.01 \pm 1.04$	28245	26396
M33	73206	52455	11049	47594	0	$-0.09 \pm 1.09$	$0.11 \pm 1.12$	$0.04 \pm 1.17$	71847	71847
Phoenix Dwarf	10831	0	499	0	1212	$0.01 \pm 0.87$	$0.35 \pm 0.95$	$-0.19 \pm 0.95$	10703	10021
NGC 1313	6156	6156	481	6156	6156	$0.27 \pm 1.36^*$	$0.06 \pm 1.41^*$	$0.45 \pm 1.14^*$	5970	5970
NGC 2366	495	156	64	0	0	$-0.16 \pm 1.12^*$	$0.09 \pm 1.15^*$	$-0.13 \pm 1.27^*$	462	462
NGC 2403	16644	3735	1517	0	0	$-0.01 \pm 1.43$	$0.26 \pm 1.64$	$-0.05 \pm 1.47$	15936	15910
M81	28479	3894	1072	0	0	$-0.16 \pm 1.12^*$	$0.09 \pm 1.15^*$	$-0.13 \pm 1.27^*$	27895	27875
Sextans B	4914	1166	141	0	0	$-0.16 \pm 1.12^*$	$0.09 \pm 1.15^*$	$-0.13 \pm 1.27^*$	4852	4413
NGC 3109	9474	2988	1069	0	0	$-0.09 \pm 0.93$	$-0.01 \pm 1.06$	$-0.05 \pm 1.18$	8939	8935
NGC 3077	2617	271	90	0	0	$-0.16 \pm 1.12^*$	$0.09 \pm 1.15^*$	$-0.13 \pm 1.27^*$	2548	2548
Sextans A	2888	880	219	0	355	$0.03 \pm 0.84$	$-0.20 \pm 0.98$	$-0.12 \pm 0.94$	2848	2693
NGC 4214	1159	368	95	89	0	$-0.16 \pm 1.12^*$	$0.09 \pm 1.15^*$	$-0.13 \pm 1.27^*$	1149	1149
NGC 4736	10043	1248	349	657	0	$-0.16 \pm 1.12^*$	$0.09 \pm 1.15^*$	$-0.13 \pm 1.27^*$	9861	9861
NGC 4826	4659	480	149	306	0	$-0.16 \pm 1.12^*$	$0.09 \pm 1.15^*$	$-0.13 \pm 1.27^*$	4577	4575
M 83	15020	2422	1396	0	3877	$-0.04 \pm 0.76$	$0.31 \pm 1.20$	$0.07 \pm 1.05$	14132	14132
NGC 5253	721	0	119	0	187	$-0.16 \pm 1.12^*$	$0.09 \pm 1.15^*$	$-0.13 \pm 1.27^*$	622	622
NGC 6822	25599	18659	7061	0	15205	$0.01 \pm 1.13$	$-0.08 \pm 1.05$	$-0.24 \pm 1.16$	22483	22471
Pegasus DIG	11316	2234	251	0	0	$-0.16 \pm 1.12^*$	$0.09 \pm 1.15^*$	$-0.13 \pm 1.27^*$	11147	10530
NGC 7793	5535	887	353	0	0	$0.04 \pm 1.47$	$0.09 \pm 1.32$	$-0.04 \pm 1.06$	5433	5425

**Notes.** *Spitzer* data for galaxies IC 10, IC 1613, Pegasus DIG, Phoenix Dwarf, Sextans A and B, and WLM are derived from [Boyer et al. \(2015\)](#); M33, M81, NGC 2403, NGC 247, NGC 300, NGC 6822, and NGC 7793 from [Khan et al. \(2015\)](#); NGC 2366, NGC 253, NGC 4214, NGC 5253, and NGC 55 from [Williams & Bonanos \(2016\)](#); M31, M81, NGC 3077, NGC 4736, NGC 1313, and NGC 4826 from [Khan \(2017\)](#). <sup>(\*)</sup> For those galaxies the parallax and proper motion criteria derived from M31 were used, as there were not enough data to determine these quantities by using their data only.





- Fig. 1. Example of the fitting processing and foreground removal in NGC 2403.
- Top panel: Gaia sources where the green ellipse defines the boundary selected for the galaxy.
- Middle panel: Fitting the parallax data for all sources within NGC 2403.
  - the foreground contribution (dark gray dotted line) is scaled according to the densities of sources inside and outside the galaxy
  - the purple dashed line shows the (Gaussian) contribution of galactic sources
  - the blue line indicates the total fit
  - the vertical black dashed lines show the  $3\sigma$  limits defined by the Gaussian properties of the galactic sources.
- Bottom panel: Similar to parallax, but for proper motion in declination.

## 2. Data collection and processing

- 2.4. Quality cuts
  - Class: BSG - a rather loose class of early-type and hot stars, YSG - evolved yellow type stars, RSG - red supergiants, BeBR - B[e] supergiants, LBV - Luminous Blue Variables, WR - Wolf-Rayet stars, GAL - galaxies including AGNs and background QSOs (i.e. all extragalactic outliers).
  - The probability per class is provided for each of the algorithms used (i.e. Support Vector Machines, Random Forest, Multi-Layer Perceptron), which are then combined (with equal weighting) to provide the final set of probabilities.
  - We opted to use a cut at **0.66**.

# 3. Results

## • 3.1. Catalog description

- In the Table we provide the source ID, Spitzer coordinates, Gaia DR3 ID, proper motion and parallax, Spitzer, PS1, and near-IR photometry and errors, previous classification (if available), probabilities per class for each method including the ensemble one, as well as final class, final probability, and band completeness.

**Table 3.** Final source catalog with predicted classifications for all galaxies.

ID	R.A. (J2000) (deg)	Dec. (J2000) (deg)	<i>Gaia</i> _DR3_ID	...	Final_Class	Final_Prob	Band_Compl
WLM-2	0.52017	-15.44622	—	...	WR	0.602	1.0
WLM-3	0.52012	-15.40681	—	...	WR	0.647	0.4
WLM-4	0.52012	-15.36033	—	...	RSG	0.859	1.0
WLM-5	0.52012	-15.46578	—	...	WR	0.618	0.2
WLM-7	0.52012	-15.44331	—	...	WR	0.648	0.2
WLM-8	0.52012	-15.41617	—	...	WR	0.574	0.2
WLM-9	0.52008	-15.50714	—	...	WR	0.612	0.2
WLM-10	0.52008	-15.46256	—	...	WR	0.536	0.2
WLM-11	0.52008	-15.56622	—	...	WR	0.438	0.6
WLM-12	0.52008	-15.42581	—	...	WR	0.615	0.2
WLM-13	0.52008	-15.43997	—	...	WR	0.613	0.2
WLM-14	0.52008	-15.54617	—	...	WR	0.558	0.2
WLM-16	0.52008	-15.56514	—	...	RSG	0.396	0.2
WLM-17	0.52004	-15.53664	—	...	YSG	0.476	0.6
WLM-18	0.52004	-15.55456	—	...	WR	0.473	0.2
WLM-19	0.52000	-15.40131	—	...	WR	0.430	0.6
WLM-21	0.52000	-15.46006	—	...	WR	0.646	0.2
WLM-22	0.52000	-15.60042	—	...	WR	0.615	0.2
WLM-24	0.51996	-15.45511	—	...	WR	0.616	0.2
WLM-25	0.51996	-15.35928	—	...	RSG	0.487	0.2

# 3. Results

## • 3.2. Populations

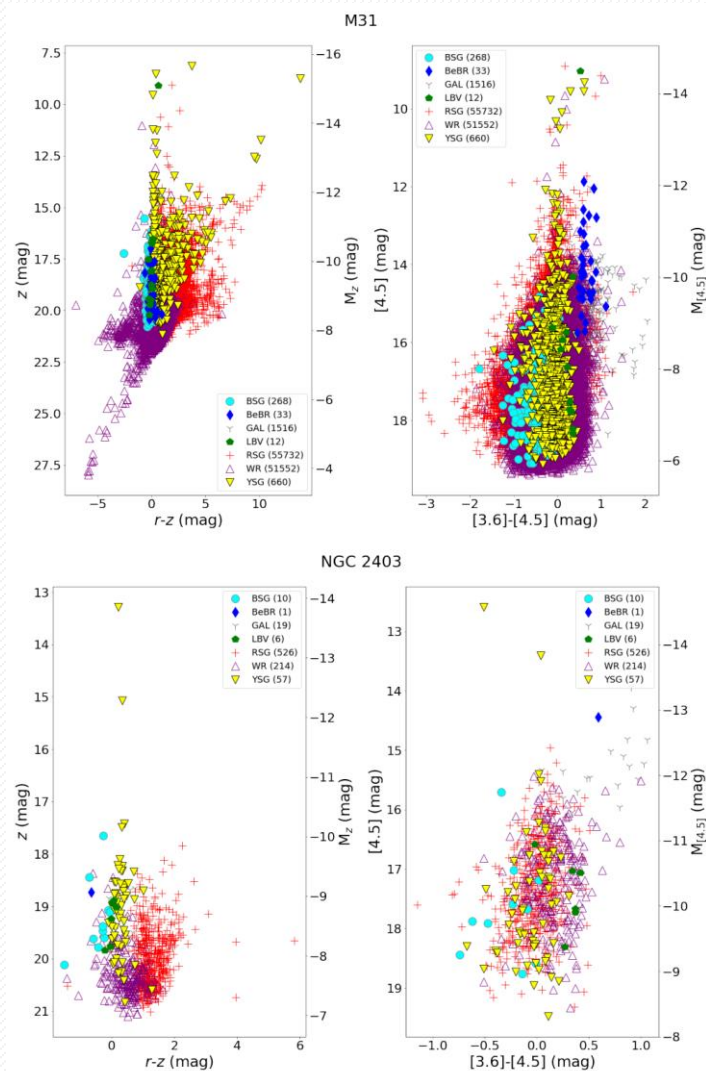
- Table 4 presents the total number of source classifications, along with the number of predictions for the classes of RSG, YSG, BSG, BeBR, WR, LBV, and GAL, independently.
- Overall, the highest number of predictions to be for RSGs and WR stars. In particular, M31, M33, NGC 6822, IC 1613, IC10, and M81 have more than 1000 classified sources.

**Table 4.** Number of predictions per galaxy, after applying the selection criteria on probability and band completeness (from Sect. 2.4).

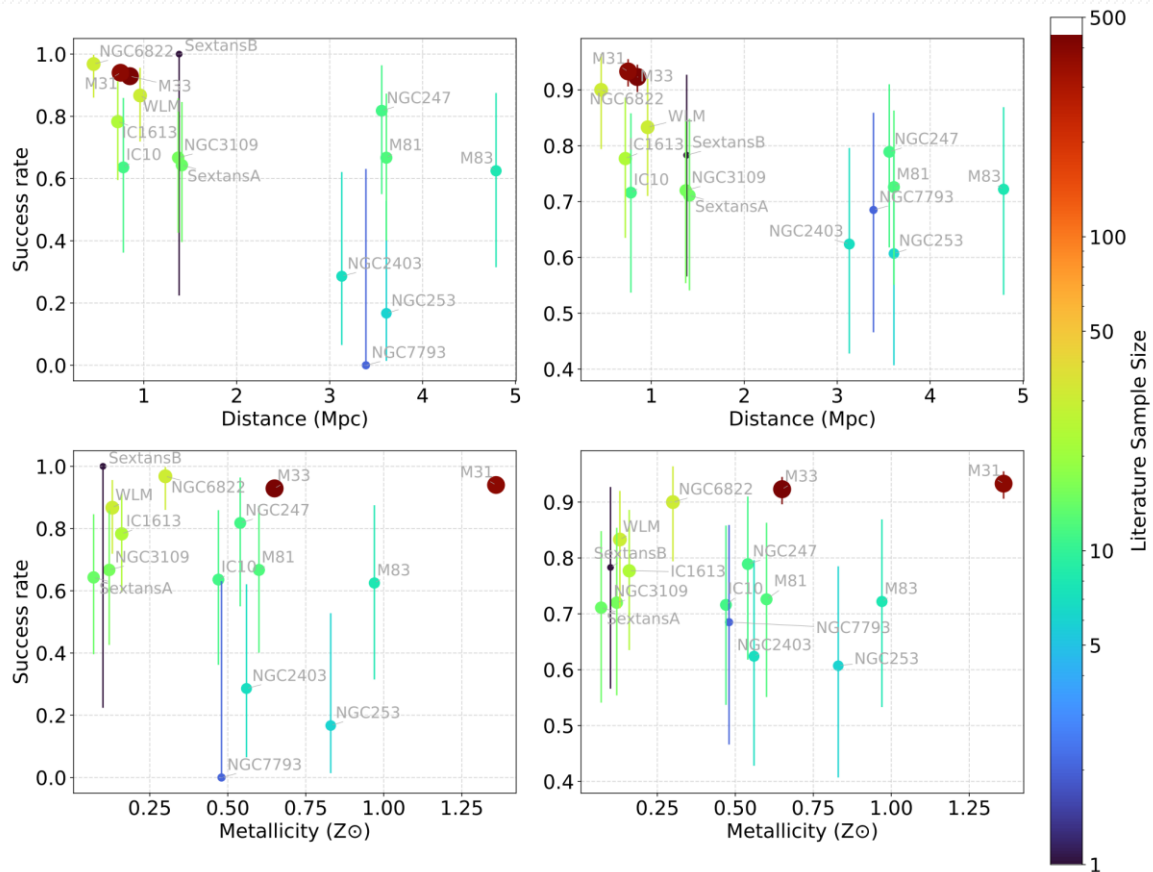
Galaxy	Total	RSG	YSG	BSG	BeBR	WR	LBV	GAL
WLM	526	268	85	13	2	147	1	10
IC 10	1622	658	11	0	0	947	0	6
M31	225176	81734	696	268	33	140153	12	2280
NGC 247	897	372	17	6	0	423	1	78
NGC 253	385	167	36	1	1	118	5	57
IC 1613	2964	2351	392	39	1	162	5	14
M33	31635	25808	322	212	23	4767	8	495
NGC 2366	42	29	5	0	0	2	0	6
NGC 2403	950	620	74	10	1	217	6	22
M81	1387	382	36	1	2	899	1	66
Sextans B	231	176	25	2	0	24	0	4
NGC 3109	736	363	38	7	0	319	1	8
NGC 3077	96	17	1	0	0	68	0	10
Sextans A	168	100	20	8	0	35	2	3
NGC 4214	142	42	10	4	0	81	0	5
NGC 4736	341	49	30	0	1	227	0	34
NGC 4826	151	24	19	0	0	94	0	14
M83	565	104	28	10	4	388	1	30
NGC 6822	8007	6992	220	34	4	690	17	50
Pegasus DIG	627	217	15	1	0	389	0	5
NGC 7793	9	6	2	0	0	1	0	0
TOTAL	276657	120479	2082	616	72	150151	60	3197

# 3. Results

- 3.3. Color-Magnitude Diagrams
  - Fig. 2 shows optical and mid-IR CMDs for two example galaxies, M31 and NGC 2403.
  - The position of sources matches their predictions. In the  $z$  vs.  $r - z$  CMD we see BSG located on the left (of approximately  $r - z \sim 0$ ) while YSG and RSG extend to redder colors as expected. The few BeBR and LBV predicted are located (consistently) close to the BSG and WR.
  - Regarding the  $[4.5]$  vs.  $[3.6] - [4.5]$  CMD we notice that the majority of the RSGs lie around  $[3.6] - [4.5] \sim 0$  mag in both M31 and NGC 2403, consistent with what we would expect.
  - Overall, the position of the sources matches their predicted classification. a fraction of sources that is misclassified. This is due to a number of physical and technical reasons.



# 4. Discussion

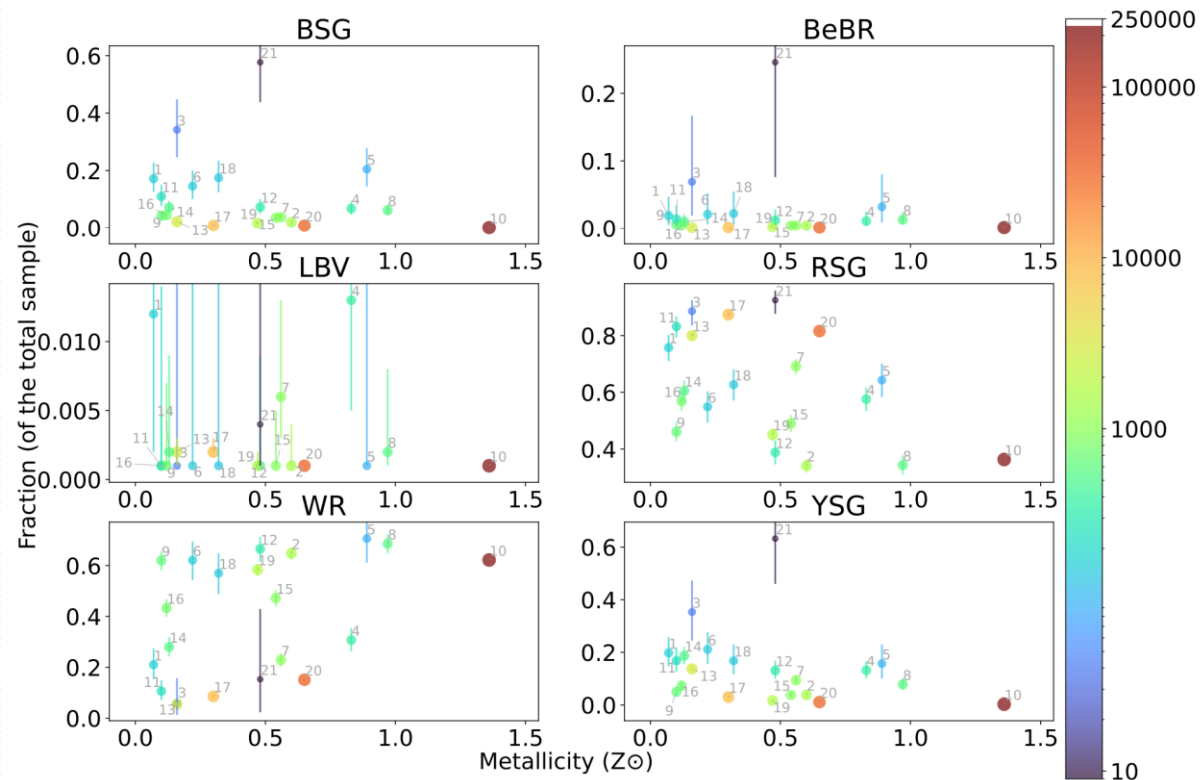


- Fig. 3. Success rate vs. distance (top panels) and metallicity (bottom panels), using a uniform prior (left panels) and a unimodal beta distribution (right panels) with a peak corresponding to  $77 \pm 7\%$  (based on the performance of the classifier during developing).
- The number of available classified sources from the literature is indicated by the size of the points and the color bar on the right.
- We notice a small decrease of the success rate with distance and a relatively flat behavior with metallicity, especially in the case where a prior is implemented .



# 4. Discussion

1: Sextans A 2: M81 3: NGC 2366 4: NGC 253 5: NGC 3077 6: NGC 4826 7: NGC 2403 8: M83 9: Pegasus DIG 10: M31 11: Sextans B  
12: NGC 4736 13: IC 1613 14: WLM 15: NGC 247 16: NGC 3109 17: NGC 6822 18: NGC 4214 19: IC 10 20: M33 21: NGC 7793



- Fig. 4. The fraction of predicted population with metallicity per class.
- We investigated the effect of metallicity on different stellar populations, finding expected trends, such as a decrease in WR stars at lower metallicities and a relative increase in BSGs and YSGs.
- However, a number of selection biases, among which Spitzer's sensitivity to dusty evolved stars, must be considered when interpreting these trends.
- The symbol size and color for each galaxy reflects the corresponding sample size.

## 4. Discussion

- Luminous RSGs
  - In **M31**, the three most luminous sources (close to  $\log(L/L_{\odot}) \sim 7$ ; IDs: M31-439614, M31-439351, and M31-439254) do not have a Gaia counterpart, which means that these could be foreground red stars.
  - The next most luminous source (ID M31-350) is a confirmed M1 I RSG (J004428.48+415130.9), with a range of  $\log(L/L_{\odot}) = 5.43\text{--}5.64$  [\*McDonald et al. \(2022\)\*](#).
  - 12 sources (between  $\log(L/L_{\odot}) \sim 5.8 - 5.5$ ), of which 3 have Gaia parallax and proper motion values

## 4. Discussion

- Luminous RSGs
  - In **M33**, we find two sources (M33-179 and M33-520) at  $\log(L/L_{\odot}) \sim 6$ . Since both of them lack Gaia parallax and proper motion measurements (but have photometric measurements) we cannot determine if they are genuine M33 members or not.
  - Source M33-173 at  $\log(L/L_{\odot}) \sim 5.7$ , for which full Gaia information exists. However, this is a known OB star ([\*Massey et al. 2016\*](#)) and marks an erroneous prediction as a RSG.
  - Another source (ID M33-646) has only Gaia photometry and, therefore, we can only tentatively consider it as a M33 RSG.
  - The remaining two sources have full Gaia information, and have been classified spectroscopically as RSGs.

# 5. Summary

- In this study, we presented a comprehensive catalog of massive stars across 26 galaxies within 5 Mpc, leveraging a machine learning classifier trained on optical and infrared photometry.
- Our classifier successfully classified 1,147,650 sources, of which 276,657 were deemed robust classifications based on probability and completeness criteria. Among these, we identified 120,479 RSGs, 2082 YSGs, 616 BSGs, 72 B[e] Supergiants, 150,151 WR stars, and 60 LBVs.
- A key result of our study is the effectiveness of the classifier across a broad metallicity range ( $0.07\text{--}1.36\ Z_{\odot}$ ), demonstrating its applicability even at low metallicities ( $\sim 0.1\ Z_{\odot}$ ), despite not being explicitly trained for such environments. The classifier remains robust at distances  $\leq 1.5$  Mpc, with only a slight decline beyond 3 Mpc due to the spatial resolution limits of Spitzer.
- We investigated the effect of metallicity on different stellar populations, finding expected trends, such as a decrease in WR stars at lower metallicities and a relative increase in BSGs and YSGs.
- We also identified 21 luminous RSGs ( $\log(L/L_{\odot}) \geq 5.5$ ), including 6 extreme RSGs in M31 ( $\log(L/L_{\odot}) \geq 6$ ), challenging the Humphreys-Davidson limit. Further investigation of these sources is necessary to confirm their nature and more accurately determine their luminosity.
- Furthermore, we compiled a catalog of 5,273 spectroscopically confirmed sources for all the 26 galaxies as derived from the literature. This offers a unique dataset of reference regarding spectral types for all massive stars and candidates known so far (including additional  $\sim 330$  other sources).

